RESEARCH ARTICLE

UV assisted photo reactive polyether-polyesteramide resin for future applications in 3D printing

Steffi I. Macías[1] | Guillem Ruano[1] | Núria Borràs[1] | Carlos Alemán[1,2] | Elaine Armelin[1,2]

[1]Departament d'Enginyeria Química, EEBE, Universitat Politècnica de Catalunya, Barcelona, Spain

[2]Barcelona Research Center for Multiscale Science, EEBE, Barcelona, Spain

Correspondence

Carlos Alemán and Elaine Armelin, Departament d'Enginyeria Química, EEBE, Universitat Politècnica de Catalunya, C/d'Eduard Maristany, 10-14, 2nd floor, 08019 Barcelona, Spain.
Emails:
Email: carlos.aleman@upc.edu (C. A.) and
Email: elaine.armelin@upc.edu (E. A.)

Abstract

Among additive manufacturing, photocuring 3D printing technologies are very relevant because of its high printing speed and high precision. However, the limited performance of photosensitive thermoset polymers is the bottleneck for the application of photocuring 3D printing in some fields, particularly in the biomedical sector. Thus, the development of biodegradable and biocompatible materials is highly desirable and of utmost importance. In this work, a biodegradable and non-cytotoxic thermoset polymer for photocuring 3D printing is reported. It consists of an unsaturated polyesteramide bearing phenylalanine, 2-butene-1,4-diol and fumarate building blocks, which is photocured under UV irradiation using a low molecular weight poly(ethylene glycol) diacrylate as crosslinker. The main characteristics of the new thermoset are: (1) very high volumetric and mechanical integrity stabilities, comparable to that of photocured epoxies; (2) very high degradation temperature; (3) very low water absorption capacity; (4) relatively fast enzymatic degradation, reaching 16.5% after 3 months; and (5) non-cytotoxic response in presence of epithelial cells, even when soluble molecular fragments coming from biodegradation are considered. These properties favor the future utilization of the new polyether-polyesteramide resin in the manufacturing of more sustainable products via 3D printing methods, such as stereolithography, that uses UV sources.

KEYWORDS

acrylate resins, biodegradability, polyesteramide, UV curing

1 | INTRODUCTION

Additive manufacturing (3D printing) technologies to make polymeric spatial objects has experienced growth in multiple scientific and technological fields.[1–3] Stereolithography (SLA) technology, which is based on a layer-by-layer photopolymerization process and was the first proposed 3D printing concept,[4] currently allows printing objects with high precision and smooth surface at high printing speed.[5–7] Advances have also been developed in other photocuring 3D printing techniques, such as digital light processing (DLP), continuous liquid interface production (CLIP) and two-photon 3D printing (TPP), which differ among them in the pattern formation and the principle of control system.[8]

Unlike the thermoplastics used in extrusion 3D printing technologies, like fused deposition modeling (FDM), photosensitive polymers are thermoset plastics. Thus, once the photocuring chemical reaction takes place to harden the material, it cannot be re-melted. Although they can include a number of ingredients, such as pigments, colorants, plasticizers and optical absorbers, the key elements necessary for photocuring 3D printing techniques are photoinitiators, and reactive oligomers and monomers.[9] At the end, photosensitive resins used for photocuring 3D printing are chosen as a function of the wavelength of the lamp (i.e., UV or visible light to cure a thin layer of liquid sample) and the printing technology (i.e., SLA, DLP, among others). SLA printing is the most popular photocuring 3D printing technique because of its time efficiency, high resolution, and easy accessibility.[10–12] On the other hand, high energy UV light is usually preferred because it provides rapid polymerization processes, even though visible light offers safety and an environment that is benign to living cells for tissue engineering applications.[13,14] Acrylates and urethanes are among the most frequently used thermoset plastics for SLA.[15–18]

A common characteristic of all photocuring 3D printing technologies is that printed objects are frequently employed as temporary materials, being discarded after a short period of usage. As 3D printed thermoset plastics cannot be directly recycled due to their crosslinked nature, development of biodegradable materials for photocuring 3D printing is currently a priority. In a pioneering work Matsuda et al.[19] introduced the concept of photocurable liquid biodegradable copolymers for photoconstructs. However, the amount of biodegradable photopolymerizable thermoset plastics is not only very scarce but also very specific for biomedical applications (e.g., tissue engineering).[6,20–23] In this context, the development of biodegradable and biocompatible photocuring thermoset plastics is especially attractive since they could be used for both biomedical and technological application, while preserving the commitment to the environment.

In this work we propose a biodegradable and biocompatible thermoset plastic for photocuring 3D printing that is based on a photo-crosslink unsaturated polyesteramide (UPEA), which contains phenylalanine, 2-butene-1,4-diol and fumarate as building blocks.[24] Polyesteramides typically combines the excellent properties of polyamides with the degradability and biocompatibility of polyesters. Incorporation of unsaturated double bonds to polyesteramides provides capacity to afford crosslinking or functionalization reactions, depending on their positions.[25] The first issue afforded in this study was to probe the successful formation of a stable thermoset plastic by photocrosslinking the UPEA oligomer with a short poly(ethylene glycol) diacrylate (M_n = 250 g/mol), with UV light irradiation. For this purpose, the obtained thermoset, hereafter named PEG250-UPEA, was compared with the blank achieved by photocuring the poly(ethylene glycol) diacrylate alone (i.e., without UPEA) using the same experimental conditions, the resulting product being named PEG250. After this, studies have been focused on the study of the biodegradability of PEG250-UPEA.

2 | METHODS

2.1 | Materials

Reagents were used as purchased without further purification. L-phenylalanine (reagent grade, 98%), p-toluenesulfonic acid monohydrate (ACS reagent, 98.5%), cis-2-butene-1,4-diol (97%), toluene (99.8%), fumaryl chloride (95%), acetone (HPLC, 99.9%), acryloyl chloride (97%), 1-butanol (ACS reagent, 99.4%), n-hexane (reagent grade) and 2-hydroxy-4′-(2-hydroxyethoxy)-2-methylpropiophenone (Irgacure) were purchased from Sigma-Aldrich and poly(ethylene glycol) diacrylate (M_n = 250 g/mol; PEG250) was purchased from Fluka.

2.2 | Synthesis of UPEA

The preparation of the di-p-toluenesulfonic acid salt of L-phenylalanine butene 1,4-diester (M1) and di-p-nitrophenyl fumarate (M2) monomers was as follows:

2.2.1 | Di-p-toluenesulfonic acid salt of L-phenylalanine butene 1,4-diester (M1)

0.038 mol of L-phenylalanine (Phe), 0.038 mol of p-toluenesulphonic acid monohydrate and 0.017 mol of butenediol were dissolved in 90 ml of toluene. The solution was heated to 135 °C and kept during at least 24 h in a Dean-Stark trap until reaching the maximum volume of distilled water (i.e., 1.5 ml; 0.0669 mol) that the condensation makes. After this, the reaction mixture was cooling down and the obtained solid was filtered, dried and re-crystalized at least three times in dimethyl sulfoxide (DMSO).

Yield: 40%. M.p.: 239 °C. IR (cm^{-1}): 1737 (O=C), 1456 (=C—H).and 1191 (COO—). ^{1}H NMR (DMSO-d_6, ppm, δ): 8.41 (s, 3H, NH$_3$), 7.46, 7.09 (dd, 5H, arom), 7.31–7.22 (m,5H, Phe), 5.54 (t, 1H, CH), 4.66 (d, 2H, CH$_2$), 4.33 (t, 1H, CH), 3.07 (m, 4H, CH$_2$), 2.28 (s, 3H, CH$_3$).

2.2.2 | Di-*p*-nitrophenyl fumarate (M2)

A 40 ml solution of fumaryl chloride (0.030 mol) in acetone was added dropwise to 100 ml of acetone with *p*-nitrophenol (0.060 mol) and triethylamine (0.060 mol) at $-78\ °C$ using an acetone and dry ice bath. The system was kept under vigorous stirring at room temperature for 24 h. The resulting product was purified by recrystallization in acetonitrile.

Yield: 70%. M.p.: 123 °C. IR (cm^{-1}):3101 (C=CH—), 1734 (C=O), 1615, 957 (—CH=CH—CO—), 1519, 1345 (–NO_2), 1212 (COO—). ^{1}H NMR (DMSO-d_6, ppm, δ): 8.34 (d, 2H, arom), 7.59 (d, 2H, arom), 7.24 (s, 1H, =CH).

2.2.3 | Unsaturated polyesteramide

1 mmol of M1 and 1 mmol of M2 were mixed in 4 ml of dry dimethylacetamide. Then, 2.2 mmol of triethylamine were added dropwise and the solution was heated to 60 °C with stirring for at least 96 h (i.e., until the complete dissolution of M1 and M2). The resulting solution was precipitated with cold ethyl acetate. The solid was filtered and extracted with ethyl acetate in a Soxhlet apparatus for 96 h, and finally dried.

Yield: 75%. M.p.: 128 °C. M_w: 60400 g/mol. PDI: 2.50. IR (cm^{-1}): 3315 (Amide A), 1736 (C=O), 1623 (Amide 1), 1530 (Amide 2), 1455 (CH_2), 1170 (COO—). ^{1}H NMR (DMSO-d_6, ppm, δ): 8.93 (d, 1H, NH), 7.22 (m, 5H, arom), 6.84 (s, 1H, CH), 5.58 (s, 1H, CH), 4.65 (s, 2H, CH_2), 4.58 (t, 1H, CH), 3.04 (m, 2H, CH_2).

2.2.4 | PEG250-UPEA thermoset polymer

0.080 g of UPEA dissolved in 0.35 ml of PEG250 were homogenized at room temperature with a magnetic stirrer for 24 h. The photoreticulation reaction was conducted by adding the photoinitiator irgacure 2959 (0.016 g, 5% wt with respect to the total mass of the precursors). The solution was exposed to an UV lamp (365 nm, 230 V, 0.8 A) with increasing time until cure. Although different photocuring times were evaluated, most of the assays displayed in this work were performed using thermoset resins obtained after 50 min of irradiation exposition. The resulting thermoset was immersed in deionized water (under magnetic stirring) for 24 h before its characterization. The preparation of the specimens for physical–chemical characterization, enzymatic degradation and biocompatibility studies was performed using Teflon molds of dimensions $2.0 \times 0.6 \times 0.3\ cm^3$.

2.3 | Instrumentation

The surface and internal morphologies of the prepared thermoset resins was examined by scanning electron microscopy (SEM) using a Focused Ion Beam Zeiss Neon40 scanning electron microscope equipped with an energy dispersive X-ray (EDX) spectroscopy system and operating at 5 kV. All samples were sputter-coated with a thin carbon layer using a K950X Turbo Evaporator to prevent electron charging problems.

Fourier-transform infrared transmittance (FTIR) spectra were recorded on a FTIR Jasco 4700 spectrophotometer, equipped with an attenuated total reflection accessory (Top-plate) with a diamond crystal (Specac model MKII Golden Gate Heated Single Reflection Diamond ATR). The samples were placed above the diamond crystal and several scans were carried out. For each sample 64 scans were performed between 4000 and 600 cm^{-1} with a resolution of 4 cm^{-1}. For the chemical composition analysis, only one sample was evaluated. In the case of degradation study after enzymatic assay, three samples were analyzed.

Calorimetric data were obtained by differential scanning calorimetry (DSC) with a TA Instruments Q100 series equipped with a refrigerated cooling system (RCS) operating at temperatures from -90 to 600 °C. Experiments were conducted under a flow of dry nitrogen with a sample weight of approximately 5 mg, calibration being performed with indium. The T_{zero} calibration requested two experiments: the first was done without samples while the second one was performed with sapphire disks. Heating runs were performed at 20 °C/min. Determination of T_g values from the calorimetric curves was carried out with the TA-Universal Analysis software furnished with the instrument. Thermal degradation was determined at a heating rate of 20 °C/min with around 5–8 mg samples in a Q50 thermogravimetric analyzer of TA Instruments and under a flow of dry nitrogen. Analyses were performed in the temperature range from 50 to 600 °C.

Static water contact angle (WCA) measurements with the sessile drop method were recorded using deionized water drops and analyzed at room temperature on an OCA-15EC contact angle meter from DataPhysics Instruments GmbH with SCA20 software (version 4.3.12 build 1037). The sessile drop was gently put on the surface of the samples using a micrometric syringe with a proper metallic needle (Hamilton 500 μl). The ellipse method was used to fit a mathematical function to the measured drop contour. For each system, 20 drops were examined.

The rheological behavior of the liquid resin was evaluated with a rheometer Discovery HR-2 (TA Instruments)

equipped with parallel plate geometry (20 mm of diameter). The analysis was performed at a controlled temperature of 23 °C, a 500 μm gap and a shear rate ranging from 0.1 to 100 s^{-1}.

The mechanical properties of PEG250 and PEG250-UPEA thermosets were evaluated through stress–strain assays by using a Zwick Z2.5/TN1S testing machine. Specimens of dimensions 20 mm of length, 5 mm of width and 2 mm of thickness were obtained after UV curing (procedure described in the section 2.2.4) in Teflon molds. The deformation rate was 10 mm·min^{-1}. All the mechanical parameters reported in this work were obtained by averaging the results obtained from three independent measurements.

2.4 | Enzymatic degradation

Enzymatic degradation studies were carried out placing hydrogel samples (100 mg) in vials containing 0.1 mg/ml of lipase *Rhizopus oryzae* in a 5 ml of phosphate buffer saline (PBS) solution supplemented with 0.1 mg/ml of sodium azide to prevent contamination. Samples were incubated at 37 °C in a shaking incubator set at 100 rpm for a total of 3 months. Vials were closed and sealed with parafilm to avoid loss of solution by evaporation, even though the PBS solution was replaced every 48 h. The variation of the weight loss against the exposure time was used to evaluate the enzymatic degradability from a quantitative point of view. For this purpose, samples (in triplicate) were removed at predefined interval times, frozen, lyophilized and weighted. Degradation was quantitatively monitored as weight loss (WL, in %) of the samples by applying the following formula:

$$WL = \frac{m_0 - m_t}{m_0} \times 100 \qquad (1)$$

where m_0 is the weight of the sample before the degradation assay and m_t is the weight of the sample after exposure to the degradation medium. The influence of the enzymatic degradation on the morphology was evaluated by SEM and FTIR.

2.5 | Cytotoxicity assays

The cytotoxicity of thermoset polymer extracts from biodegradation was evaluated using the MDCK-SIAT1 (Canine Cocker Spaniel Kidney Sialic Acid Over Expression) cell line, which exhibits epithelial morphology. These cells were routinely grown in DMEM high glucose medium buffered with 2.5 mM of 4-(2-hydroxyethyl)-

1-piperazineethanesulfonic acid (HEPES), 10% fetal bovine serum (FBS), penicillin (100 units/ml), and streptomycin (100 μg/ml). The cultures were maintained in a humidified incubator with an atmosphere of 5% CO_2 and 95% O_2 at 37 °C. Culture media were changed every 2 days. When the cells reached 80–90% confluence, they were detached using 2 ml of trypsin (0.25% trypsin/EDTA) for 5 min at 37 °C. Finally, cells were re-suspended in 5 ml of fresh medium and their concentration was determined by counting with a Neubauer camera using 0.4% trypan blue as a vital dye.

Survival assays were performed with the extracts obtained at 1, 3, 6, 9, 12 and 15 days of collection. Briefly, MDCK-SIAT1s were seeded in 96-well plates (tissue culture polystyrene, TCPS) at the density of 20,000 cells/well and cultured overnight to adhere. The cells were then incubated for 24 h in 100 μl medium containing PEG250-UPEA or PEG250 (blank) extracts concentrated or diluted four times (1% methanol). A PBS solution, like that used for enzymatic degradation assays, was used in order to serve as control.

3 | RESULTS AND DISCUSSION

3.1 | Synthesis of the PEG250-UPEA thermoset resin

The synthesis of the two monomers necessary for the preparation of the UPEA was adapted from Katsarava and coworkers.[24] The first monomer is the di-*p*-toluenesulfonic acid salt of ʟ-phenylalanine butene 1,4-diester (**M1** in Scheme 1A; yield: 40%), while the second is the di-*p*-nitrophenyl fumarate (**M2** in Scheme 1A; yield: 70%). The polycondensation of **M1** and **M2** results in the UPEA, which bears two C=C bonds in the backbone coming from the 2-butene-1,4-diol and the fumarate building blocks (Scheme 1B), as a white solid and a yield of 75%.

The UPEA (M_w: 60400 g/mol; PDI: 2.50) was used to produce the photocured thermoset, PEG250-UPEA, using liquid poly(ethylene glycol) diacrylate of $M_n = 250$ g/mol as crosslinker (PEG250) and Irgacure 2959 as photoinitiator (Scheme 2). The advantage of using small PEG oligomers is the high reactivity in comparison to high M_w UPEA oligomer, whereas the initiator has the advantage of working at UV-A electromagnetic wavelength (365 nm, blue color), which is not supposed to degrade the samples. For this purpose, UPEA was previously dissolved with the crosslinker monomer (i.e., solvent-free synthesis) and homogenized at room temperature with a magnetic stirrer overnight (Figure 1A). Then, the photoinitiator (5 wt% with respect to the total

SCHEME 1 Synthesis of: (A) monomers M1 and M2; and (B) unsaturated polyesteramide
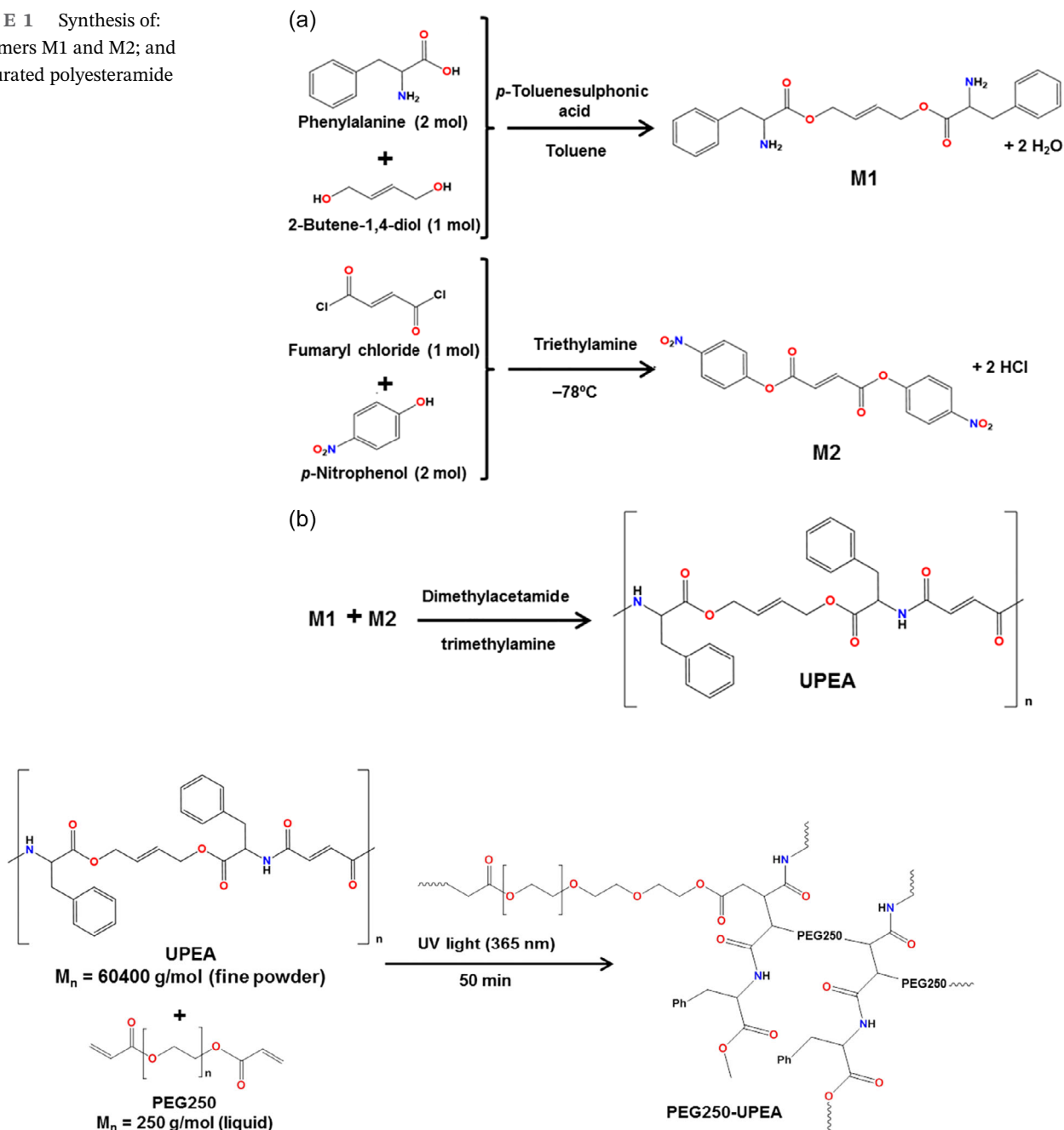
SCHEME 2 Synthesis of the PEG250-UPEA thermoset resin

mass of the precursors) was added to the mixture. The photocuring process took place in Teflon molds at room temperature, after exposition for 50 min to an UV lamp emitting at a wavelength of 365 nm.

It is worth mentioning that preliminary synthetic assays (not shown) evidenced that the time required for the photopolymerization process increased considerably with the molecular length of the crosslinker (PEG). For example, the photopolymerization time increased to more than 8 h when the crosslinker was poly(ethylene glycol) diacrylate (PEG) with $M_n = 32,600$ g/mol.

Furthermore, dimethylacetamide solvent was necessary to disperse the two solids, UPEA and PEG, which is a great problem regarding the implementation of eco-friendly syntheses. Conversely, as PEG250 is already liquid and polar enough to disperse the fine UPEA powder (Scheme 2), no solvent was needed for the dispersion of the solid UPEA, as commented above, which represents an important advantage for 3D printing technologies. Another important observation is that the aforementioned dispersion is stable over time, the mixture showed in Figure 1A remaining well homogenized for at least 3 days.
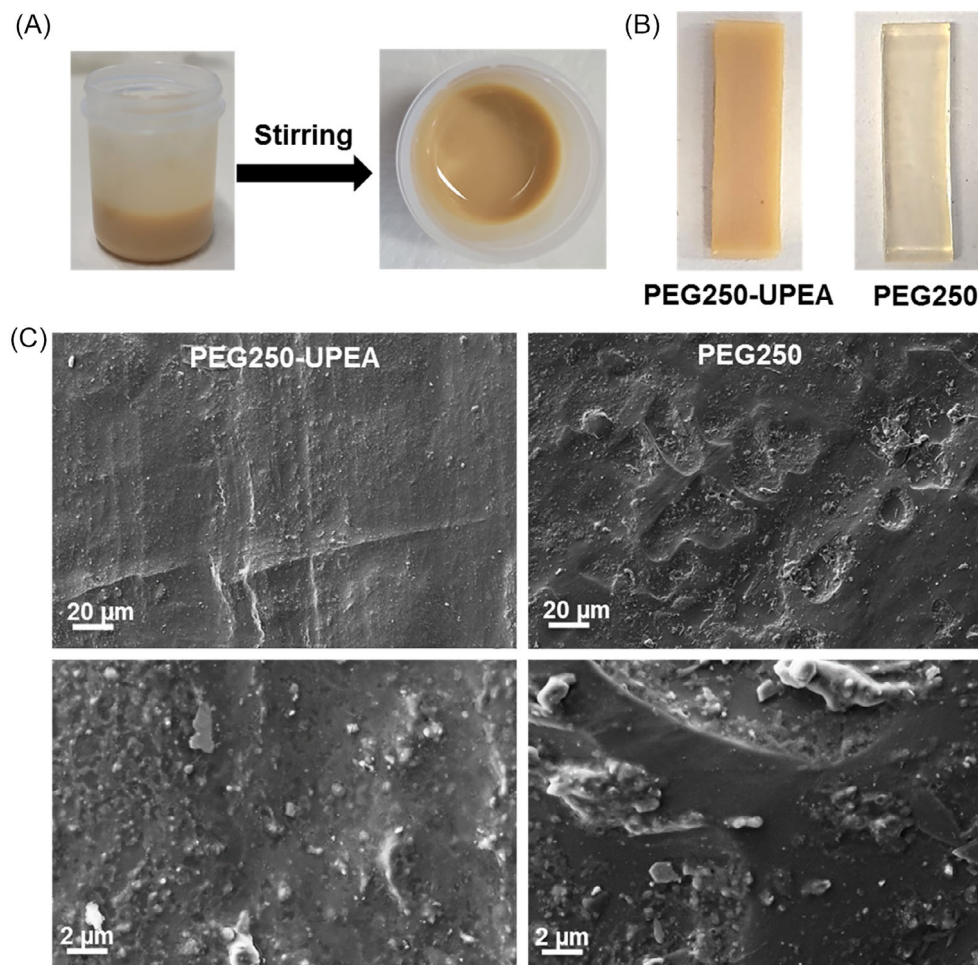
In the case of the short PEG250 crosslinker, the photocuring process was apparently completed after 50 min, as was proved by comparing with PEG250-UPEA thermoset resins obtained using higher photopolymerization times (see Figure 1 and section 2.2).

As can be seen in the Figure 1A, the mixture of liquid PEG250 with UPEA fine powder gives risen to a viscous and opaque liquid. In order to obtain smooth and perfect pieces by 3D-printing, the viscosity of the resin must stand within a certain range. If the viscosity of the resin is too low, it can likely to spread out on edges and corners of prototypes being processed before it can be cured by the UV light. The UV curable PEG250-UPEA photoresin had a higher viscosity at low shear rate ($154 \ Pa \cdot s^{-1}$ at 10^{-1} shear rate, Figure S1A) when compared to the pure PEG resin ($\sim 0 \ Pa \cdot s^{-1}$ at 10^{-1} of shear rate, Figure S1B). Even if the shear rate increases up to $100 \ s^{-1}$, PEG250 resin remains at very low viscosity parameters. As the new copolymer resin is envisaged for 3D-printing technologies, particularly SLA, the rheological properties of PEG250-UPEA ensures that the suspension is stable enough for printability.

In order to understand the effect of the presence of an unsaturated polyesteramide (bearing phenylalanine, 2-butene-1,4-diol and fumarate building blocks) in the crosslinked PEG250-UPEA thermoset, PEG250 photocured resins (blanks) were also prepared using the same procedure described in the section 2.2.4. Strips of PEG250-UPEA and PEG250 thermosets, which were prepared in Teflon rubber molds of $2.0 \times 0.6 \times 0.3 \ cm^3$, are compared in Figure 1B. PEG250 and PEG250-UPEA strips were transparent and opaque, respectively. This was attributed to the fact that in the PEG250-UPEA resin, the UPEA chains probably separate in nanosized domains, while the blank system consisted in a single phase. Therefore, the nanosized domains observed in PEG250-UPEA are the responsible for the alteration in the optical properties of pure PEG thermoset.

3.2 | Thermoset characterization

The volume shrinkage of PEG250-UPEA, which was evaluated by comparing the dimension of the designed strips (i.e., the volume inside the mold filled with the liquid mixture) and the dimension of the strip after the photocuring process, was of $3.8 \pm 1.8\%$ only. The
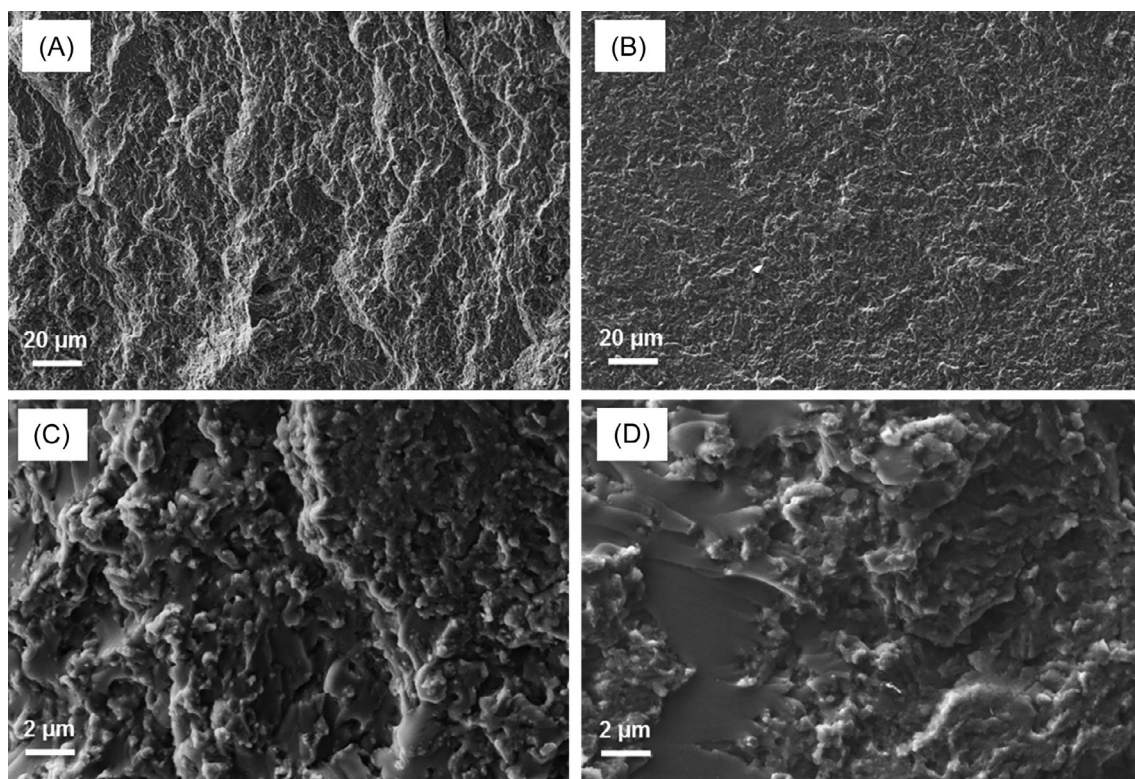
FIGURE 2 SEM micrographs of the cross-section of PEG250-UPEA thermoset specimens obtained after: (A) 50 min and (B) 110 min of photo curing. Images from (C and D) were obtained by high magnification of SEM micrographs showed in (A) and (B) figures. SEM, scanning electron microscopy; UPEA, unsaturated polyesteramide

shrinkage and the associated internal stress, which originates from the conversion of van der Waals interactions to covalent bonds,[26] might result in bending and deformation during the photocuring 3D printing fabrication. The volumetric shrinkage observed for PEG250-UPEA is comparable to that of photocured epoxide monomers, which are much appreciated because of their volumetric stability, and significantly lower than that of traditional acrylate systems ($\sim$14%).[27]

The surface morphology of PEG250-UPEA and PEG250 are compared in Figure 1C. Although SEM micrographs reveal some morphological differences, which were attributed to the presence or not of UPEA, both resins show a very compact structure, which is consistent with a complete photoreticulation reaction at the surface. Indeed, the surface morphology and compactness of PEG250-UPEA did not change with increasing photocuring time. This is illustrated in Figure S2, which displays SEM topography images of the PEG250-UPEA resin obtained after expand the photocuring time to 110 min. On the contrary, comparison of the SEM cross-section images of PEG250-UPEA specimens exposed to the UV light for 50 and 110 min reveals some differences (Figure 2). Thus, the distribution of globular structures at different levels is much more uneven and pronounced for

the former resin than for the latter one, whereas the distribution of practically flat domains is more prominent for resin obtained using the largest photocuring time. These morphological characteristics indicate that, although the reticulation degree at the surface is similar for the samples obtained using a photoreticulation time of 50 and 110 min, the internal photocuration degree of PEG250-UPEA increases with time. This feature is consistent with the opaque nature of the material, hindering for UV radiation to reach the inner core. Although this could be interpreted as a limitation for the applicability of PEG250-UPEA in photocuring 3D printing, it is not. This is because the photo-cured layer thickness in such technologies typically ranges from 10 to 100 μm and cannot be obstructed by the light irradiation.

The chemical composition and crosslinking reaction were followed by FTIR-ATR technique. Figure 3 compares the absorption bands of PEG250-UPEA and PEG250 thermoset polymers with those of pristine UPEA and PEG250 crosslinker. The individual spectra of the raw material are supplied in the ESI (Figure S3).

The absorption bands associated to the C=C vinyl end group of PEG250 crosslinker, which appear at 1634, 1407 and 808 cm^{-1}, were used to check the progress of polymerization reaction. A reduction of such bands was
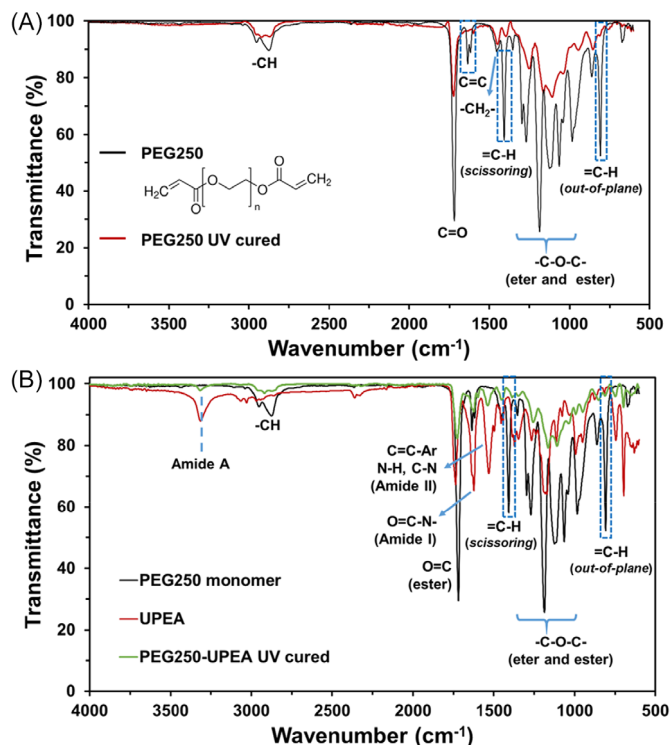
FIGURE 3 FTIR spectra of: (A) PEG250 crosslinker and PEG250 thermoset polymer cured with UV-light for 50 min, and (B) unsaturated polyesteramide (UPEA), PEG250 crosslinker and PEG250-UPEA cured with UV-light for 50 min

associated to the enhancement of photoreticulation reaction. Figure 3A proves that the PEG250 monomers were completely reacted by the action of UV light after 50 min forming the PEG250 thermoset polymer. On the other hand, FTIR analyses of the photochemical reaction between UPEA and PEG250 showed some problems associated with overlapping bands. More specifically, the absorption band at 1634 cm^{-1} overlaps with the C=C of aromatic rings from UPEA, while that of 1407 cm^{-1} coincides with C—N polar groups. Moreover, due to the structure of the UPEA repeating units (Scheme 1B), the =C—H alkyl groups has not the same vibration intensity than vinyl =C—H end groups from PEG250 crosslinker. Fortunately, the crosslinker absorption band at about 808 cm^{-1} is strong and sharp enough to be used as reference. Accordingly, Figure 3B shows the comparison of raw materials and the final PEG250-UPEA thermoset polymer after UV curing of 50 min. The latter presents absorption bands from both UPEA (Amide A, 3312 cm^{-1}; ester, 1733 cm^{-1}; Amide I, 1625 cm^{-1}, among others) and the three sharp bands from ester of PEG250 crosslinker (1160, 1107 and 1033 cm^{-1}). The largest difference with respect to the crosslinker molecules is the significant reduction of the absorption bands from =C—H acrylate end groups (1407 and 808 cm^{-1}) from PEG.

DSC thermograms of PEG250-UPEA and PEG250 resins photocured during 50 min are displayed in Figure 4A,B. The inflection showed in the curve at 45 and 49 °C for PEG250-UPEA and pure PEG250, respectively, is attributable to the initial glass transition temperature (T_g). Furthermore, both resins show some exothermic events that may indicate some residual activity. In the second heating scan, the glass transition temperature ($T_{g,\infty}$) increased to 59 and 74 °C for PEG250-UPEA and PEG250, respectively, and the exothermic events disappeared, indicating that the residual reactivity was almost suppressed. This can be explained as the result of the increased crosslink density caused by the thermal curing induced in the first scan.

Thermogravimetic analysis (TGA) results are displayed in Figure 4C,D. The thermal degradation of the crosslinked PEG250-UPEA occurs in three main steps, as is reflected by the first derivative of the TGA (DTGA) curve (Figure 4C). In the first step, a mass loss of ~3% is observed at around 210 °C, which has been attributed to non-reacted PEG molecules that had not been incorporated to the crosslinked network. This is in agreement with SEM micrographs of samples obtained using different photoreticulation times (Figure 2). The second step, which occurs at around 347 °C, corresponds to the degradation of the UPEA main chain, that is, present in smallest proportion with respect to PEG molecules. Finally, the third step at 439 °C has been mainly associated to the degradation of the crosslinks-containing segments. This is consistent with the thermal degradation of PEG250 resins, which exhibit a single step at 431 °C. The lack of oligomers in PEG250 TGA curve is fully consistent with the single one step degradation observed in Figure 4D.

Previous studies reported the fabrication of polyesteramide hydrogels (UPEA-h) prepared using large chains of poly(ethylene glycol) diacrylate (PEG, M_w: 10000 g/mol) as crosslinker[28] and their utilization as solid electrolytes for electrochemical supercapacitors when doped with NaCl.[29] An intrinsic property of such hydrogels, hereafter named PEG-UPEA/h, was the high water absorption capacity (i.e., swelling ratio, SR). Thus, the SR of PEG-UPEA/h, which was estimated using the weights of the hydrogel after washing and after freeze-drying, ranged from 500 ± 114% to 1501 ± 342%, depending with on crosslinking degree (i.e., the SR decreased with increasing reticulation degree).[30] Both the complete crosslinking achieved in the present work for PEG250-UPEA and the reduction of the crosslinker length from a polymer (PEG, M_w: 10000 g/mol) to a short oligomer (PEG, M_w: 250 g/mol) allow the formation of a solid thermoset polymer rather than a semi-solid hydrogel. The SR for the PEG250-UPEA resin, which was
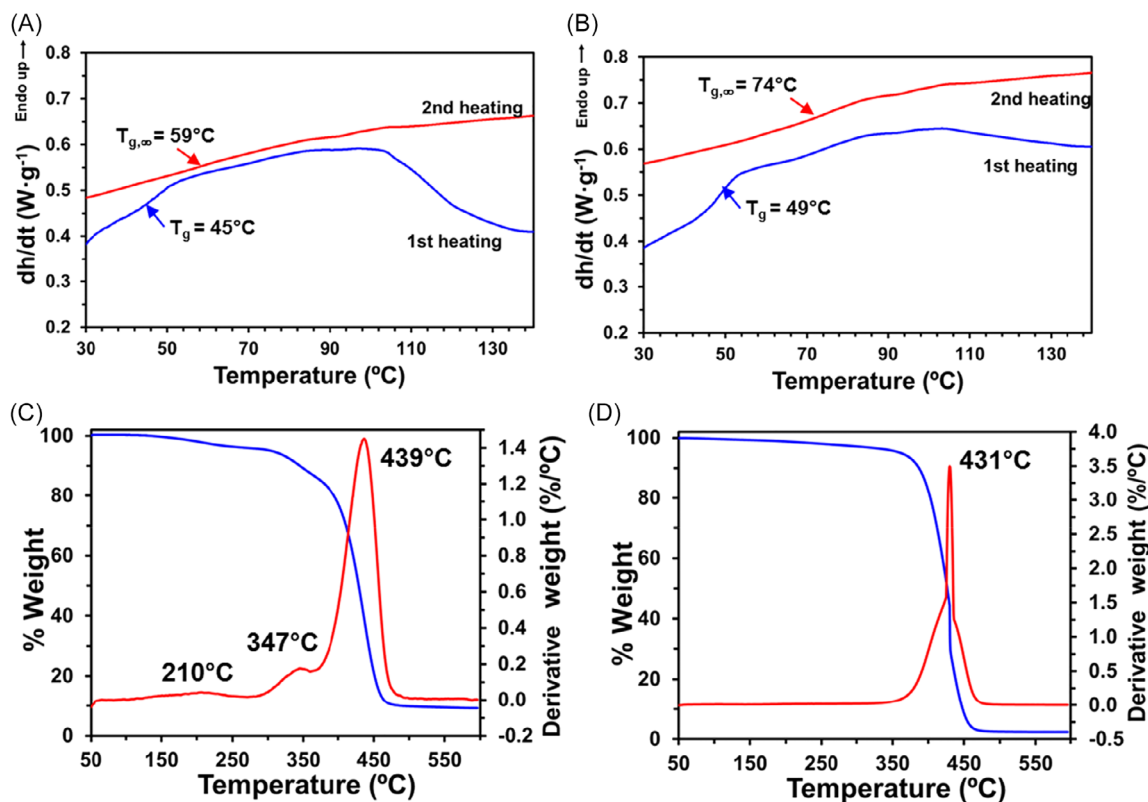
FIGURE 4   (A, B) DSC thermograms of first heating and second heating traces and (C, D) TGA and DTGA curves of (A, C) PEG250-UPEA and (B, D) PEG250 thermoset resins. DSC, differential scanning calorimetry; DTGA, derivative of the TGA; TGA, thermogravimetic analysis; UPEA, unsaturated polyesteramide

determined using the same methodology, was found to be only $3.8 \pm 0.6\%$, representing a compact and solid structure. Consistently with the well-known water affinity of amide and ester bonds, this value is higher than that obtained for the PEG250 resin ($0.8 \pm 0.2\%$).

Moreover, the wettability of PEG250-UPEA and PEG250 surfaces was measured by dropping a deionized water droplet over the surface and determining the WCA. After considering different areas of the surface during the measurement, the average WCAs determined were $86 \pm 1°$ and $83 \pm 4°$ for PEG250 and PEG250-UPEA thermoset polymers, respectively, indicating the slight hydrophilicity of their surfaces. Then, the small addition of UPEA units does not affect the wettability of the UV cured resin.

To investigate the mechanical integrity of the new thermoset copolymer, stress–strain measurements were performed and compared to pure PEG250 homopolymer. After UV curing process both samples presented similar mechanical properties, as expected, due to the low percentage of UPEA present in the PEG250-UPEA sample (Figure S4). The Young's modulus varied from 153.8 ± 23.4 MPa to 135.8 ± 28.4 MPa, respectively, in PEG250 (Figure S4A) and PEG250-UPEA (Figure S4B)

thermosets. The maximum strength value was also inferior for the copolymer (106.5 ± 9.0 MPa) than for the homopolymer (132.2 ± 5.7 MPa). The slight lower elastic modulus and tensile strength of the copolymer is explained by the higher mobility that UPEA chains impart to the whole system. It is also well-known that thermoset polymers do not have high elongation at break if the polymer is well crosslinked. In our example, both systems presented very low strain percentages ($0.80 \pm 0.14\%$ and $0.78 \pm 0.10\%$, for PEG250 and PEG250-UPEA, respectively).

3.3 | Biodegradability

Polyesters, which are extensively used for biomedical, biotechnological and agricultural applications, exhibit excellent biodegradability.[30–32] Thus, polymer chains are degraded into small soluble fragment by hydrolase enzymes excreted from the microorganisms in the medium (e.g., lipases and esterases), which cleavage the hydrolysable ester bonds. Thus, esters bonds are expected to be responsible of the PEG250-UPEA biodegradability. In general, polyesteramides biodegradability increases
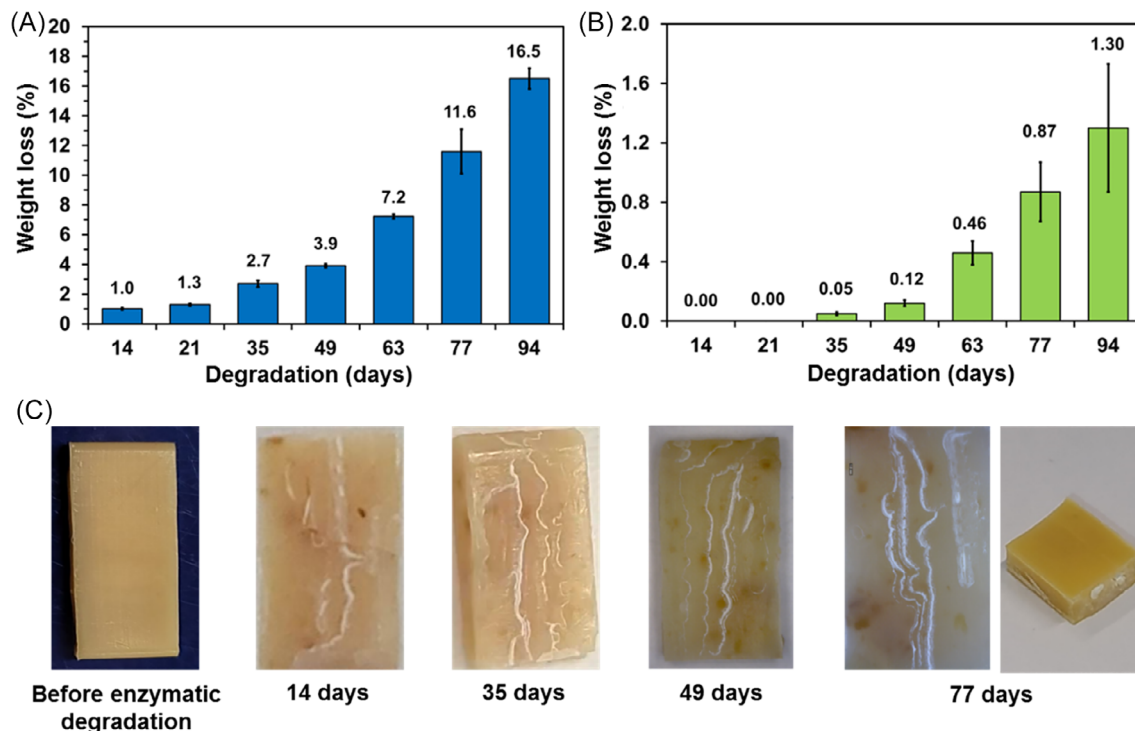
FIGURE 5 (A) Normalized weight loss of PEG250-UPEA (in %) as a function of the time of incubation in the enzymatic solution. (B) Macroscopic photographs of the surface of PEG250-UPEA strips, extracted at different time intervals, where clear fissures are observed after 14 days of enzymatic degradation. (C) Normalized weight loss of PEG250 (in %) as a function of the time of incubation in the enzymatic solution. UPEA, unsaturated polyesteramide

with ester content[25] and decreases with increasing crystallinity.[33] In the case of PEG250-UPEA, phenylalanine units and crosslinks are expected to reduce the crystallinity with respect to polyester thermosets and thermoplastics, respectively, facilitating the cleavage of the ester bonds. In this work, the biodegradation of PEG250-UPEA and PEG250 (blank) was investigated using lipase from *Rhizopus oryzae*, which is frequently employed for in vitro enzymatic degradation studies due to its high stability and activity.[34,35] Samples were incubated under shaking at 37 °C in a lipase-containing PBS solution for 3 months. The biodegradation process was monitored by the weight loss, which is indicative of the hydrolysis of polymer chains into soluble fragments, and by FTIR spectroscopy and SEM techniques.

Figure 5 illustrates the weight loss of the resins with prolonged degradation time. The weight loss of PEG250-UPEA was $2.7 \pm 0.2\%$, $7.2 \pm 0.2\%$ and $16.5 \pm 0.7\%$ after 1, 2 and 3 months of enzymatic hydrolysis, respectively, evidencing a relatively fast biodegradation rate (Figure 5A). Indeed, the biodegradation rate grew following an exponential behavior, evidencing that the activity of the enzyme to change the polyesteramide molecules into oligomers and segments of low molecular weight rapidly increased with time. This feature suggests that,

after attack the surface and the corners of the tested samples, the enzyme penetrated and cleaved ester bonds located at the inner regions of the samples. Thus, after surface erosion, the enzymatic digestion gave place to a rough and non-uniform surface, with cracks, cavities and pits, as is shown in Figure 5B. However, the fact that the visual aspect of the samples did not experienced very pronounced changes after 35 days while the weight loss increased exponentially, confirms that the enzyme penetrates inside the samples degrading the ester linkages at their internal parts. This statement, which was demonstrated by SEM cross-section analysis (see below), was also supported by naked eye inspection of the cross-section of intentionally broken samples, which exhibit clear signs of degradation (Figure 5B) after 77 days in contact with the degradation medium. Conversely, in the control experiments using PEG250 samples, the weight loss after 3 months of immersion in the enzymatic buffer solution was lower than 1% (Figure 5C), which corroborates the beneficial presence of UPEA chains to promote the biodegradability of the new thermoset material.

SEM micrographs, which are compared in Figure 6, corroborate the degradation mechanism proposed for PEG250-UPEA. More specifically, the enzyme affects the surface morphology of the thermoset samples, causing the
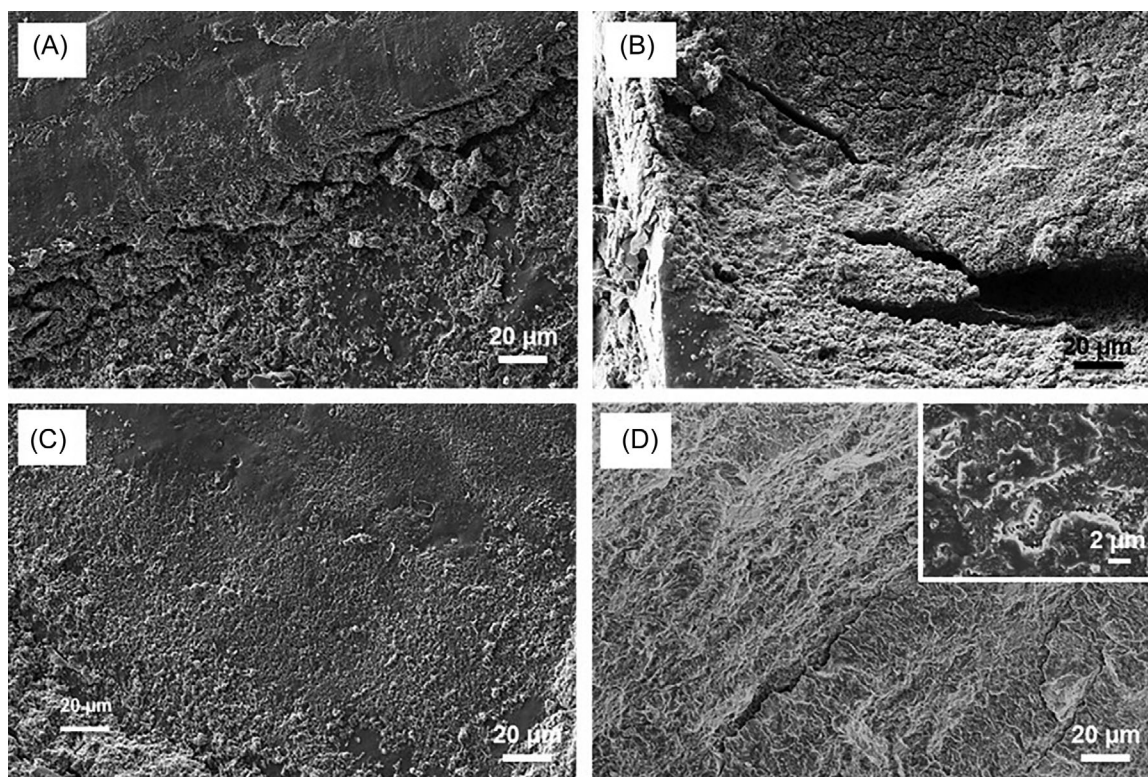
FIGURE 6 SEM micrographs of PEG250-UPEA immersed in the enzymatic solution for (A, C) 35 days and (B, D) 77 days: (A, B) topography micrographs and (C, D) cross-section micrographs. The inset (D) exhibit the irregular surface obtained after the cryo-fracture of the sample with InLens detector. SEM, scanning electron microscopy; UPEA, unsaturated polyesteramide

apparition of cavities and cracks. Although the dimensions (i.e., length, width and depth) of these elements increase with the immersion time, the superficial morphology does not exhibit important changes after 35 days. This is evidenced in Figure 6A,B, which compare samples immersed in the enzymatic solution for 35 and 77 days, respectively. The growing of the elements caused by enzymatic degradation facilitates the attack of the enzyme at the inner part of the samples. Accordingly, inspection of SEM cross-sectional images of samples incubated for 35 and 77 days (Figure 6C,D, respectively) revealed that the morphology of the former is very similar to that of pristine samples (Figure 2), whereas the latter shows crack, caves and deformations. Additional SEM micrographs of PEG250-UPEA samples immersed for 77 days, which are consistent with the penetration of the enzymes into the internal regions, are shown in Figure S5.

To certify that the biodegradation comes from polymer chains and not from mechanical stress, the cleavage of the ester bonds was monitored by FTIR and the results are shown in Figure 7. It compares the spectra of PEG250-UPEA as prepared and biodegraded after 77 days of immersion in the enzymatic medium. The peak intensities at 1252, 1160, 1107 and 1033 cm^{-1} (C—O—C in the ester bonds) decreased after such period,
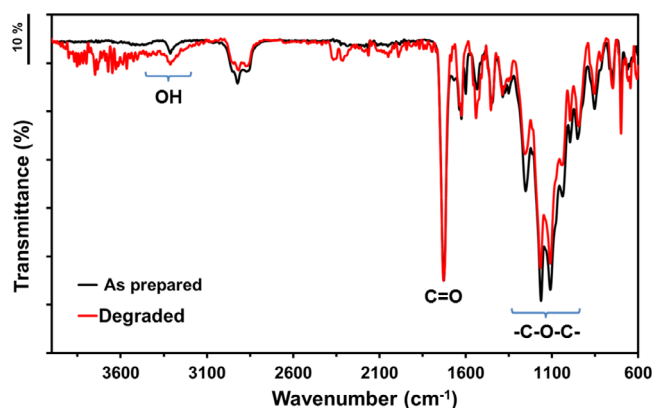
FIGURE 7 FTIR spectra of PEG250-UPEA thermoset polymer as prepared and after enzymatic degradation (77 days of immersion in a lipase containing solution). UPEA, unsaturated polyesteramide

corroborating the lipase-induced cleavage of the ester bonds. The peaks appeared in the 3500–3600 cm^{-1} interval reflect the generation of sub-products with hydroxyl groups. Although further analyses (^{1}H-NMR and ^{13}C-NMR) would be necessary to certify such statement, these analyses were discarded due to the fact the cured resin is not soluble in the solvents usually employed for NMR analyses.

3.4 | Citotoxicity

Biodegradable PEG250-UPEA thermoset plastic seems promising for photocuring 3D printing to specific applications, like disposable molds for other printing and plastic processing methods. Moreover, if it is biodegradable and non-toxic, the range of possibilities of applications in the biomedical field is highly desirable.

It was therefore appropriate to check if it presents any cytotoxicity with epithelial cells after enzymatic degradation. In our previous study,[28] the biocompatibility assays with similar copolymer (UPEA-h) in epithelial cells (Vero and MDCK-SIAT1) demonstrated a preference of cell adhesion and proliferation of MDCK-SIAT1 cell line. Therefore, in the present work, such cells were cultured for 24 h in the presence of extracts obtained at various sampling times along thermoset biodegradation in the enzymatic media, which ranged from 24 h to 15 days. As it was expected, the PEG250 thermoset (blank) behaved as the control due to its lack of biodegradability, that is, the cell viability percentage of PEG250 extracts is very similar to the TCPS plates with the solution medium (Figure 8). These assays indicated no cytotoxicity to MDCK-SIAT1 cells in presence of the thermoset resin extracts, whatever the time of biodegradation. Although a relative survival rate greater than 70% could be considered non-toxic, the viability of the MDCK-SIAT1 cells (i.e., the cell proliferation in the presence of extracts from PEG250-UPEA after immersion in the enzymatic media) was higher than 100% (Figure 8). Besides the percentage of UPEA in PEG250 crosslinker is very low, the positive

effect of the presence of ester-amide and the phenylalanine groups is clear. Close inspection of samples extracted after 15 days, leads to the conclusion that PEG250-UPEA is more biocompatible with MDCK-SIAT1 epithelial-like cells, being 26 and 15% less toxic than TCPS control and PEG250, respectively. These results indicate that the supposedly unreacted crosslinker and products released from PEG250-UPEA biodegraded samples did not induce cytotoxicity, which is an important aspect to have into account if the final objective is the processing of more biodegradable and biocompatible thermoset resins for 3D printing technologies.
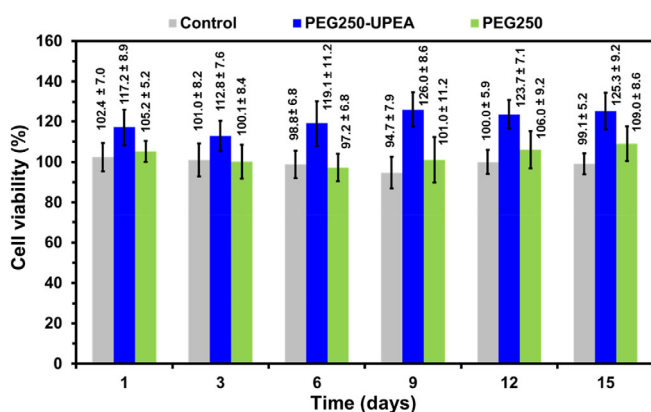
4 | CONCLUSION

The development of biodegradable and biocompatible photopolymerizable thermosets has gained considerable attention in recent years. Thus, the availability of this kind of materials is essential to extend once and for all the use of photocuring 3D printing technologies to biomedical and technological applications, preserving the commitment to the environment. This work presents a photocured thermoset derived from an unsaturated polyesteramide phenylalanine, 2-butene-1,4-diol and fumarate building blocks and short poly(ethylene glycol) diacrylate units, which were photo-cured under UV irradiation by adding a commercial initiator. In addition of low water adsorption capacity and high volumetric and thermal stabilities, PEG250-UPEA exhibits high biodegradability and low cytotoxicity to epithelial cells after biodegradation. Our findings regarding this new UV-thermoset material is expected to be useful in photocuring 3D printing technologies for biomedical and engineering prototyping. Therefore, future experiments with PEG250-UPEA resin and UPEA oligomer derivatives in SLA printer are envisaged.

FIGURE 8 Bar plot showing the cell viability of extracts taken from solutions in which PEG250-UPEA and PEG250 (blank) thermoset polymers were immersed in the enzymatic degradation medium for a number of days. All samples were compared to the control, corresponding to TCPS plates with PBS solution. PBS, phosphate buffer saline; TCPS, tissue culture polystyrene; UPEA, unsaturated polyesteramide

DATA AVAILABILITY STATEMENT
Data is available upon request to the corresponding authors.

ORCID

Núria Borràs https://orcid.org/0000-0002-4015-6611
Carlos Alemán https://orcid.org/0000-0003-4462-6075
Elaine Armelin https://orcid.org/0000-0002-0658-7696

REFERENCES

[1] J. Savolainen, M. Collan, *Add. Manufact.* **2020**, *32*, 101070.
[2] D. Chimene, R. Kaunas, A. Gaharwar, *Adv. Mater.* **2020**, *32*, 1902026.
[3] A. du Plessis, C. Broeckhoven, I. Yadroitsava, I. Yadroitsev, C. H. Hands, R. Kunju, D. Bathe, *Add. Manufact.* **2019**, *27*, 408.
[4] US4575330A, Apparatus for production of three-dimensional objects by stereolithography. C.W. Hull (3D Systems Inc.), 1986.
[5] K. Niendorf, B. Raymaekers, *Adv. Eng. Mater.* **2021**, *23*, 2001002.
[6] F. P. W. Melchels, J. Feijen, D. W. Grijpma, *Biomaterials* **2010**, *31*, 6121.
[7] M. B. A. Tamez, I. Taha, *Addit. Manufact.* **2021**, *37*, 101748.
[8] P. Fiedor, J. Ortyl, *Materials* **2020**, *13*, 2951.
[9] H. Gong, M. Beauchamp, S. Perry, W. Steven, T. Adam, G. P. Nordin, *RSC Adv.* **2015**, *5*, 106621. https://pubs.rsc.org/en/content/articlelanding/2015/ra/c5ra23855b
[10] Z. Weng, Y. Zhou, W. Lin, T. Senthil, L. Wu, *Compos. Part A Appl. Sci. Manuf.* **2016**, *88*, 234. https://www.sciencedirect.com/science/article/abs/pii/S1359835X16301725
[11] Y. Li, L. Zheng, S. Peng, J.-T. Miao, J. Zhong, L. Wu, Z. Weng, *ACS Appl. Mater. Interfaces* **2020**, *12*, 4917.
[12] L. J. Tan, W. Zhu, K. Zhou, *Adv. Funct. Mater.* **2020**, *30*, 2003062. https://onlinelibrary.wiley.com/doi/abs/10.1002/adfm.202003062
[13] A. Bagheri, J. Jin, *ACS Appl. Polym. Mater* **2019**, *1*, 593. https://pubs.acs.org/doi/abs/10.1021/acsapm.8b00165
[14] H. Kadry, S. Wadnap, C. Xu, F. Ahsan, *Eur. J. Pharm. Sci.* **2019**, *135*, 60.
[15] S. C. Ligon-Auer, M. Schwentenwein, C. Gorsche, J. Stampfl, R. Liska, *Polym. Chem.* **2016**, *7*, 257. https://pubs.rsc.org/en/content/articlelanding/2016/py/c5py01631b
[16] H. Gojzewski, Z. Guo, W. Grzelachowska, M. G. Ridwan, M. A. Hempenius, G. Grijpma, J. Vancso, *ACS Appl. Mater. Interfaces* **2020**, *12*, 8908.
[17] J. S. Manzano, H. Wang, I. I. Slowing, *ACS Appl. Polym. Mater* **2019**, *1*, 2890. https://pubs.acs.org/doi/abs/10.1021/acsapm.9b00598
[18] T. Zhao, R. Yu, X. Li, B. Cheng, Y. Zhang, X. Yang, X. Zhao, Y. Zhao, W. Huang, *Eur. Polym. J.* **2018**, *101*, 120. https://www.sciencedirect.com/science/article/abs/pii/S0014305718300600
[19] T. Matsuda, M. Mizutani, S. C. Arnold, *Macromolecules* **2000**, *33*, 795. https://pubs.acs.org/doi/abs/10.1021/ma991404i
[20] S. A. Skoog, P. L. Goering, R. J. Narayan, *J. Mater. Sci.: Mater. Med.* **2014**, *25*, 845.
[21] K.-W. Lee, S. Wang, B. C. Fox, E. L. Ritman, M. J. Yaszemski, L. Lu, *Biomacromolecules* **2007**, *8*, 1077.
[22] F. P. W. Melchels, J. Feijen, D. W. Grijpma, *Biomaterials* **2009**, *30*, 3801.
[23] J. Y. Chen, J. V. Hwang, W. S. Ao-Ieong, Y. C. Lin, Y. K. Hsieh, Y. L. Cheng, J. Wang, *Polymer* **2018**, *10*, 1263.
[24] K. Guo, C. C. Chu, E. Chkhaidze, R. Katsarava, *J. Polym. Sci., Part A: Polym. Chem.* **2005**, *43*, 1463. https://onlinelibrary.wiley.com/doi/abs/10.1002/pola.20463
[25] M. Winnacker, B. Rieger, *Polym. Chem.* **2016**, *7*, 7039. https://pubs.rsc.org/en/content/articlelanding/2016/py/c6py01783e
[26] B. Luo, Z. Fan, Z. Li, Y. Chen, Y. Tian, X. Cheng, *J. Vac. Sci. Technol., B* **2017**, *35*, 011604. https://avs.scitation.org/doi/full/10.1116/1.4973301
[27] A. Al Mousawi, F. Dumur, P. Garra, J. Toufaily, T. Hamieh, F. Goubard, T. T. Bui, B. Graff, D. Gigmes, J. Pierre Fouassier, J. Lalevée, *J. Polym. Sci., Part A: Polym. Chem.* **2017**, *55*, 1189.
[28] G. Ruano, A. Díaz, J. Tononi, J. Torras, J. Puiggalí, C. Alemán, *Polym. Test.* **2020**, *82*, 106300.
[29] G. Ruano, J. Tononi, D. Curcó, J. Puiggalí, J. Torras, C. Alemán, *Soft Matter* **2020**, *16*, 8033.
[30] I. Manavitehrani, A. Fathi, H. Badr, S. Daly, A. Negahi Shirazi, F. Dehghani, *Polymer* **2016**, *8*, 20.
[31] I. Khan, R. Nagarjuna, J. R. Dutta, R. Ganesas, *ACS Omega* **2019**, *4*, 2844.
[32] J. M. Halpern, R. Urbanski, A. K. Weinstock, D. F. Iwig, R. T. Mathers, H. A. von Recum, *J. Biomed. Mater. Res. A* **2014**, *102*, 1467.
[33] A. Díaz, R. Katsarava, J. Puiggalí, *Int. J. Mol. Sci.* **2014**, *15*, 7064.
[34] K. Shi, J. Jing, L. Song, T. Su, Z. Wang, *Int. J. Biol. Macromol.* **2020**, *144*, 183.
[35] M. T. Zumstein, D. Rechsteiner, N. Roduner, V. Perz, D. Ribitsch, G. M. Guebitz, H.-P. E. Kohler, K. McNeill, M. Sander, *Env. Sci. Technol.* **2017**, *51*, 7476.

SUPPORTING INFORMATION

Additional supporting information may be found in the online version of the article at the publisher's website.